

EOC Memo: Bandwidth Switching Progress Report #2

B. Mason
v.Sep 03, 2014

1 Summary

This report summarizes progress on testing the bandwidth-switching (BWSW) observing mode during the Austral Winter 2014 ALMA EOC campaign, following on the earlier report by J.Donovan-Meyer.

Findings:

1. Spectral window to spectral window instrumental phase stability is excellent and present no obstacle to BWSW observing.
2. However, atmospheric phase (delay) fluctuations are significantly contaminating our measurement of the SPW-to-SPW phase offsets with the current observing strategy. In fact, we find that compared to *ignoring* the SPW-to-SPW phase offsets determined by current procedures, coherence is decreased by 38% when they are applied and the map noise is increased by 60%. Therefore an appropriate observing procedure is required to measure the instrumental offsets in practice.
3. A $\sim \frac{1}{2}$ beam shift is seen in these data when the SPW offsets are applied. This needs further investigation and resolution.

Recommendations for further EOC testing:

1. Implement a short 3-scan TDM/FDM/TDM sequence to measure instrumental offsets.
2. Define one or two spectral setups that represent what is likely to be encountered in practice, with some spread in frequency, and use them in this test. I suggest a basic paradigm of: a few (4 - 16) FDMs for the science target, scattered around the receiver sidebands (include some in relatively low transmission portions of the band); with TDM's chosen in *two* ways: 1) using the same BB's as the FDM science windows; 2) using standard continuum windows. Both sidebands should be used for both science and calibration SPWs.
3. Include observations of a science target (not the phase cal) in both spectral modes so that the calibration can be fully verified.
4. Until BWSW test observations are collected that successfully meet all these criteria, focus on acquiring data at B9 or lower frequency.

2 Test Data

Test datasets are summarized in Table 1.

2.1 SPW-to-SPW Stability: BP Stability dataset

We used the BP stability dataset previously acquired (July 10, 2014; X1fa) to evaluate the stability of phases (primarily) between different base-bands (SPW 0 = BB 1 = TDM; SPW 1 = BB 1 = 58 MHz FDM; SPW 2 = BB 2 = 234 MHz FDM; SPW 3 = BB3 = 1875 MHz FDM). For this observation the spectral setup was fixed. Three bright QSOs were observed in rotation.

The data were reduced as follows:

Execution	Band	Notes
X410	B9	clean execution with FDM/TDM/TDM BP seq.
X5f3	B10	various issues; FDM/TDM/TDM BP seq.
X6fc	B10	only a few good scans, but contains a complete TDM/FDM/TDM BP seq.
X1fa	B9	July 10, 2014 BP stability test.

Table 1: Test datasets discussed in this report.

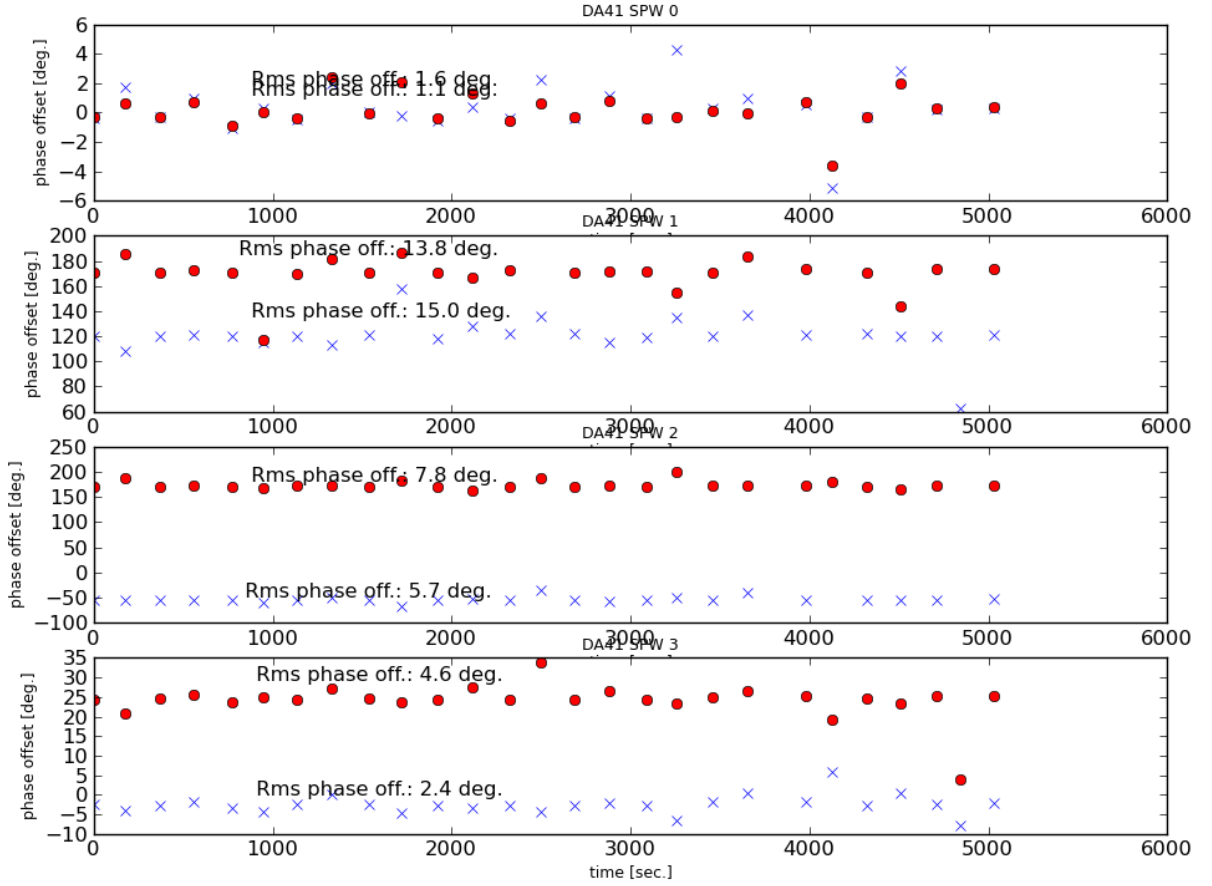


Figure 1: Typical phase offsets between SPW PHASE-INF solutions, relative to the SPW0 PHASE-INT, shown here for antenna DA41. Top panel: 2 GHz TDM window; upper middle panel: 58 MHz FDM window; lower middle panel: 234 MHz FDM window; bottom panel: 1875 MHz FDM window.

1. The script generator was used and the resulting script run on the data with no significant modifications.
2. A PHASE-INT solution (SOLINT=18.15s=6 integrations) was obtained for the TDM window on all 3 QSOs, pre-applying the BP solution (from the brightest QSO only).
3. A PHASE-INF gain solution was obtained for each source and each SPW; the BP solution was pre-applied, as was the TDM PHASE-INT solution with appropriate SPW-mapping.

An example of the resulting PHASE-INF solutions for each SPW relative to the TDM PHASE-INT solution are shown in Figure 1.

The phase solutions were extracted and analyzed, with results shown in Figure 2 (the mean offset over the execution for each ANTXPOL) and Figure 3 (the RMS and MAD¹ of phases over the execution). There are occasionally failed solutions, more common in the narrower band SPWs. Likely this is what generates the occasional outliers in phase. The RMS phase noise is also higher in the narrower FDM windows than in the wider windows, likely reflecting thermal noise in the solutions. The deviations from zero of the SPW0-SPW0 case reflect differences in the PHASE-INF and the mean value of the PHASE-INT solutions.

The SPW-to-SPW phase offsets appear very stable in time over the duration of this 1.5 hour observation, with no significant gradients evident in the solutions.

¹The Median Absolute Deviation (MAD) is a more robust estimator of the scatter in a distribution than the RMS. Here it is renormalized so that the MAD is equal to the RMS for a normal distribution.

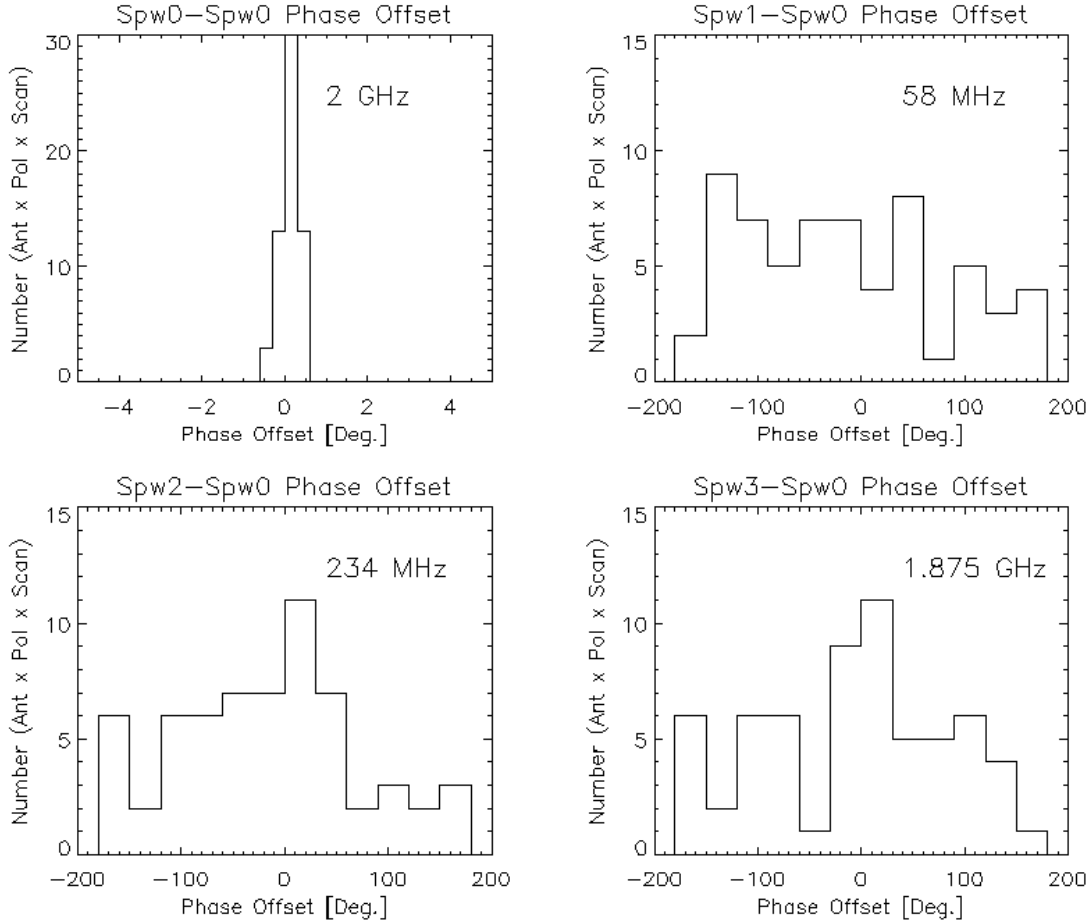


Figure 2: Distribution of SPW to SPW phase offsets.

Note that these are the *overall* phases of the SPWs. Depending on the reduction strategy the SPW-to-SPW phases derived may be smaller than this. For instance, a mean phase of each SPW is often determined from the BP observation and carried along throughout the reduction. In general it is the *stability* of the SPW-to-SPW phases that is important: here we have assessed the instrumental component of that stability. Since the various SPWs' data were collected simultaneously and the SPWs were not very different in wavelength coverage, the atmospheric delay changes with time should not be a significant effect. We assess the atmospheric effects in the next section.

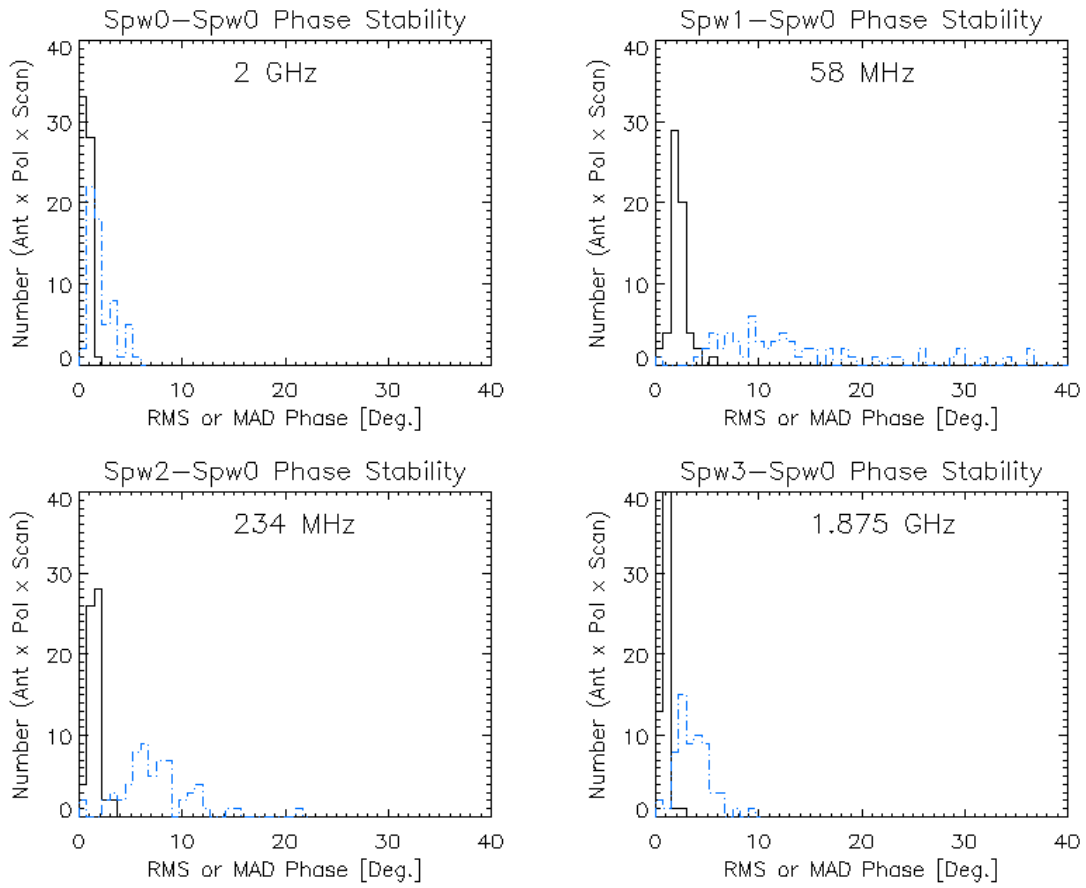


Figure 3: RMS (dashed blue) and RMS-equivalent MAD (solid black) of SPW to SPW phase offsets.

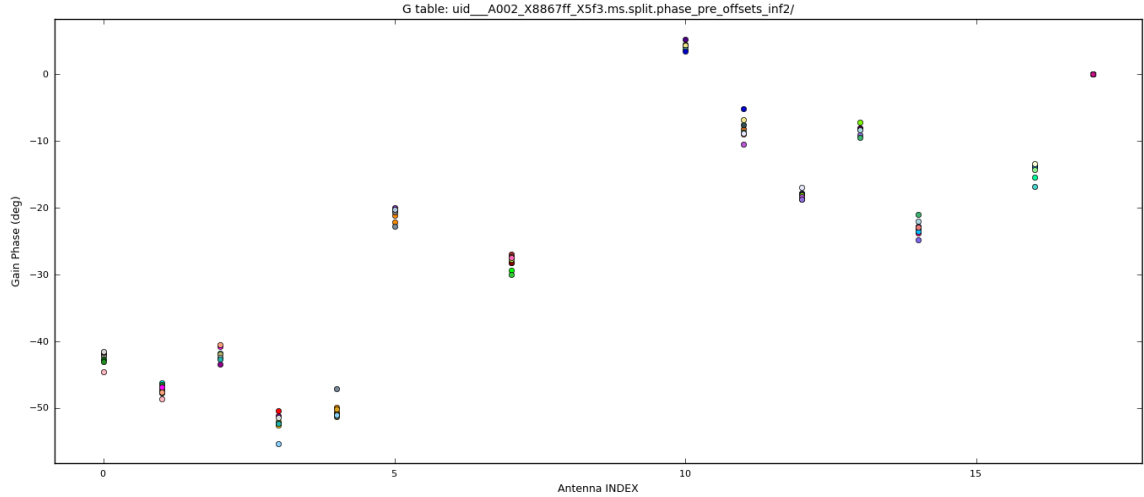


Figure 4: Difference in phase solutions for the TDM SPW for two sequential BP observations (B9, X5f3).

2.2 Atmospheric Fluctuations

Atmospheric phase/delay fluctuations are significantly affecting our attempts to measure the SPW-to-SPW offsets. This can be seen in Fig. 4 which shows a comparison of phase solutions obtained in two sequential TDM BP observations. In the absence of systematics the average TDM phases would be identical and the phase differences (plotted) would be zero.

In X6fc we obtained a TDM/FDM/TDM sequence of BP observations with the aim of being able to linearly interpolate the offset. However a bandpass observation is too long for this to be effective. This can be seen in Fig. 5 (from X410).

The BWSW observing mode will need to measure the instrumental SPW-to-SPW offsets in less than the time for atmospheric phases to change significantly.

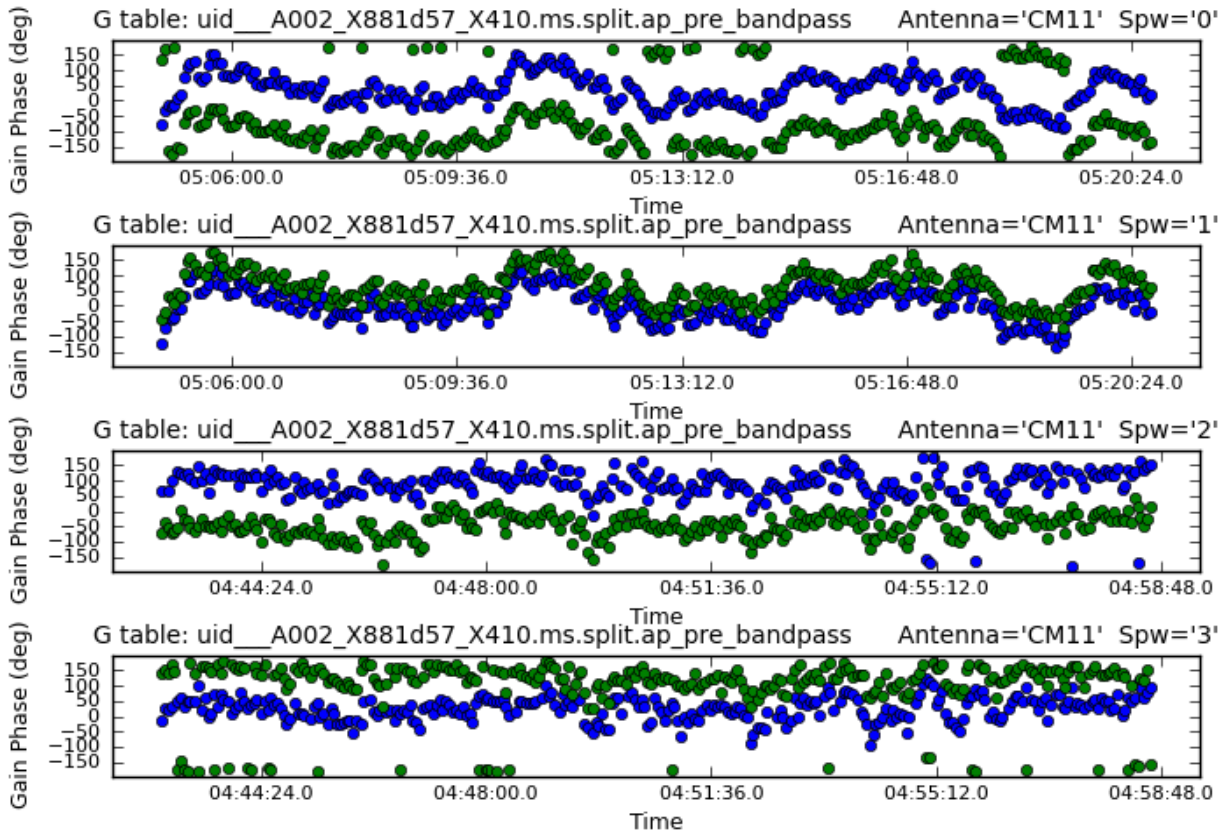


Figure 5: PHASE-INT solutions for each SPW on the BP calibrator (B9, X410) showing that phase fluctuations are large over the time period in question.

SPW	Ch0 [GHz]	BW [MHz]	Baseband
0	668.0	2000	1
1	668.0	2000	3
2	668.9	61	1
3	668.9	61	2
4	668.9	61	3
5	668.9	61	4
6	668.1	488	2
7	668.9	61	4

Table 2: SPW Setup (post-split). TDM/calibration scans used SPWs 0,1,6 & 7; science/FDM scans used SPWs 2 – 5. The SPWmap used was [0, 1, 0, 6, 1, 1, 6, 0].

2.3 Complete B9 Reduction & Imaging

The best of our test datasets is X410², the clean B9 execution obtained on July 30, 2014. This is a ~ 1.5 hr., B9 execution with ~ 0.6 mm PWV, T_{sys} values in the range 1100 – 1500 K, and a synthesized beam width of $0.24'' \times 0.16''$. The observation, in outline, proceeded as follows:

1. BP observation of 3c454.3; narrow-SPW setup; 16 minutes
2. Short BP obs. of 3c454.3; wide-SPW setup; 3 min.
3. Long BP obs. of 3c454.3; wide-SPW setup; 16 min.
4. Flux cal. on J1924-292; wide-SPW setup
5. Main observing cycle:
 - Phase cal. on J1924-292; wide-SPW setup; 30 sec.
 - Target source obs: J1923-210; narrow-SPW setup; 5 min.

The duplicate wide-SPW BP observation was inserted to check the consistency of the phase solutions. In all approximately 25 minutes of integration were collected on the target source J1923-210. The ALMA sensitivity calculator (2nd octile weather, 1155 K T_{sys} , -21° dec. source, 60 MHz BW, 668.8 GHz dual-pol, 27x12m, 10x7m) predicts 6.1 mJy/bm RMS sensitivity for the integration time achieved on this target. The SPW setup is summarized in Table 2; results presented are from SPW 4, which was referenced to SPW 1 (same BB), but results from SPWs 2 and 3 were similar.

The CASA manual script generator generated a script, but significant modifications are necessary for the script to run and calibrate the data. Modifications mostly followed the procedure reported in the first EOC BWSW report by J.Donovan-Meyer, with some tailoring of the solution intervals in time and frequency (generally increasing the amount of averaging in each). The flux and amplitude calibration were transferred directly from the TDM SPWs.

The target source was split out into its own band-averaged continuum MS. A version of the MS was also made which did *not* have the SPW-to-SPW phase offsets (table `phase_offsets_inf`) applied, since we are suspicious that these may be substantially contaminated by changes in the atmospheric delay. This “no-SPW-offs” MS did have the TDM phase-cal phase offsets applied (directly, with no correction for the differences in the SPW phases themselves).

A map of the fully calibrated dataset including the estimated SPW-to-SPW phase offsets is shown in the top left panel of Figure 6. Also shown (top right) are the residuals to a uv model fit assuming a point source model. The bottom panels show the same results after a single round of phase self-calibration using the model obtained from the UV model fit. While some residual is still evident in the map center that could likely be improved by further iterations of self-cal, the phase self-cal improves results considerably. In particular the map RMS is close to what is predicted by the sensitivity calculator and the residuals are much less strongly patterned. A map was also made from the MS with no SPW offsets. This map qualitatively resembles the post-self-cal map but with lower peak flux density.

²uid://A002/X881d57/X410

Reduction	Peak Flux [mJy/bm]	RMS Noise [mJy/bm]	Δ Position [arcsec]
SPW-offs	241	10.4	(0.07, -0.09)
”, after self-cal	462	6.5	(0.07, -0.09)
No SPW-offs	386	7.1	(0.01, -0.03)

Table 3: Imaging results for three different reduction approaches. The expected noise level from the sensitivity calculator is ~ 6.1 mJy/bm. Peak flux and position are from a uv model-fit.

Table 3 shows peak flux densities & position shifts (from `uvmodelfit`) for all three approaches— the nominal calibration, where the TDM phase-cal phases were transferred and (measured) SPW-to-SPW phase offsets applied; that, after a single round of (phase) self-cal; and result that ignore the SPW-to-SPW phase offsets. The nominal reduction retrieves only 52% of the flux that self-cal recovers; this flux is spread over the map, increasing the RMS noise by 60%. Neglecting the SPW offsets (but using the TDM phase cal solutions) does better, recovering 84% of the peak flux density. These results support the hypothesis that our measurements of the SPW-to-SPW phase offsets are significantly contaminated by atmospheric delay changes.

The peak flux obtained in the best (self-cal) case is 462 mJy/bm. The ALMA source catalog contains measurements of J1923-2104 up to 353 GHz. A power law fit to these data predicts a flux density 32% higher, 609 ± 22 mJy/bm (statistical error). Part of this discrepancy could be due to the large frequency extrapolation.

A roughly half-beam position shift is seen when the SPW phase offsets are applied; this needs to be investigated further, with better data (i.e. good measurements of the system SPW phase offsets), and SPWs spread across the receiver band (which could increase the shift). The magnitude of the shift is comparable to what was seen the earlier BWSW EOC report (Donovan-Meyer). It could be due to an atmospheric phase gradient over the array “frozen-in” to the data by our sub-optimal SPW-offset measurement procedure. It could be due to some more subtle system or CASA bug. We will want to follow this up with near-future EOC data that have better offset measurements and SPWs spread across the receiver band.

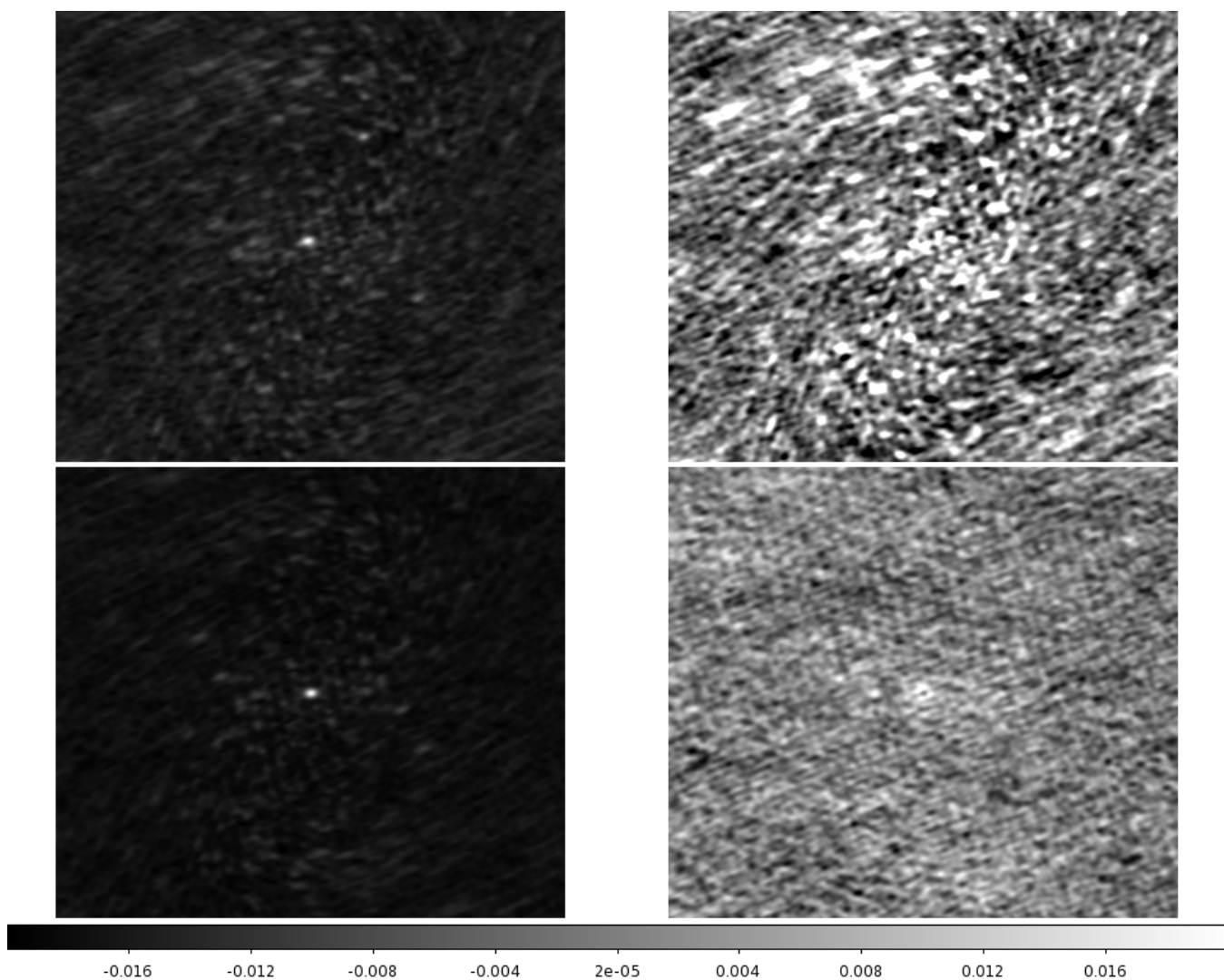


Figure 6: Dirty maps (left) and residuals to a point source uvmodelfit (right). The maps made using the full calibration procedure including application of the estimated SPW-to-SPW phase offsets applied are seen at (top); at (bottom) is the same, but after a single phase self-calibration. Dirty maps (left) are on a linear min-max scale; residual maps are on a common linear scale ranging from -20 mJy/bm to +20 mJy/bm.